

Structure-From-Motion Photogrammetry to Support the Assessment of Collapse Risk in Alpine Glaciers



**Marco Scaioni, Luigi Barazzetti, Vasil Yordanov, Roberto S. Azzoni,
Davide Fugazza, Massimo Cernuschi and Guglielmina A. Diolaiuti**

Abstract The application of Structure-from-Motion (SfM) Photogrammetry with ground-based and UAV camera stations may be exploited for modelling the topographic surface of Alpine glaciers. Multi-temporal repeated surveys lead to geometric models that may be applied to analyze the glacier retreat under global warming conditions. Thanks to the integration of point clouds obtained from ground-based and UAV imaging platforms, a complete 3D reconstruction also including vertical and sub-vertical surfaces may be achieved. These 3D models may be also exploited to understand the precursory signals of local collapse that might represent a risk for tourists and hikers visiting glaciers. In this paper a review on the application of SfM Photogrammetry in the field of glaciological studies is reported. The case of Forni Glacier in the Italian Alps is presented as emblematic study. Photogrammetric data sets obtained from measurement campaigns carried out in

M. Scaioni (✉) · L. Barazzetti
Department of Architecture, Built Environment and Construction Engineering (DABC),
Politecnico di Milano, Milan, Italy
e-mail: marco.scaioni@polimi.it

L. Barazzetti
e-mail: luigi.barazzetti@polimi.it

V. Yordanov
Polo Territoriale di Lecco, Politecnico di Milano, Milan, Italy
e-mail: vasil.yordanov@mail.polimi.it

R. S. Azzoni · G. A. Diolaiuti
Department of Environmental Science and Policy (DESP),
Università degli studi di Milano, Milan, Italy
e-mail: robertosergio.azzoni@unimi.it

G. A. Diolaiuti
e-mail: guglielmina.diolaiuti@unimi.it

D. Fugazza
Department of Earth Sciences “Ardito Desio”, Università degli studi di Milano, Milan, Italy
e-mail: davide.fugazza@unimi.it

M. Cernuschi
Agricola 2000 S.C.P.A, Tribiano, MI, Italy
e-mail: massimo.cernuschi@gmail.com

2014, 2016, 2017 and 2018 have been processed using a common workflow. Attention is paid to a few crucial aspects, such as image orientation and calibration, dense surface matching, georeferencing and data fusion. In the end, the use of output point clouds to evaluate the risk of collapse in the Forni Glacier is addressed.

1 Introduction

Global warming has resulted in severe and diffuse melting processes in the cryosphere (Kerr 2012). Alpine glaciers may be considered as the most vulnerable areas that have shown the most evident effects (Gobiet et al. 2014). By comparing the extension of continental glaciers during the last one hundred years, the glacier retreat is generally impressive. In addition, local collapsing processes have affected the terminus areas of several Alpine glaciers, very often with a very fast dynamics that led to the quick loss of important ice volumes. In the case of glaciers that are visited by tourists and mountain hikers, these local phenomena may have severe consequences on humans (Carey et al. 2015).

As thoroughly discussed in (Fugazza et al. 2018), *cryospheric hazards* include ice-avalanches from hanging glaciers (see Fig. 1), detachment of seracs, debris flows caused by the mobilization of accumulated loose sediments, water outburst that might originate from the breaching of moraines, ice-dammed lakes or collapsing englacial/subglacial systems. These processes are in general directly or indirectly accelerated under climate change forcing. In the former case, the development of proglacial moraine-dammed lakes or ice avalanches can be accounted for (see, e.g., Gobiet et al. 2014). In the latter, the retreat of permafrost



Fig. 1 Example of an ice avalanche from a hanging section of a glacier captured by the authors on Forni Glacier, Rhaetian Alps (see Sect. 3)

and glaciers may result in slope instability and in different types of landslides (see, e.g., Fey et al. 2017; Albers et al. 2017).

Moreover, glacier downwasting may affect water resources (Kääb et al. 2005b) with consequences on the local agriculture, industry and economy. The increase of glacier-related risk may have a negative influence on the tourism industry (Palomo 2017). In Fig. 2, some significant photos depicting typical risk situations that are becoming more and more frequent in places that may be easily reached by tourists and hikers are reported. These images also highlight the lack of awareness of some people visiting glacier and periglacial areas, who are not able to understand the potential risk and to maintain adequate safety measures.

Understanding under where and when a local collapse in the ice bulk may happen is not a trivial task. On one side, the direct inspection by experts who have experience of those collapsing processes in a specific region is the most valuable method to recognize the precursory signals of forthcoming collapses. On the other hand, the local reconnaissance is not always possible. Different types of sensing technologies may contribute to understand the evolution of local collapses, even though they cannot be used to establish an autonomous decision support system. The judgement by experts is always required. However, observations could help to

Fig. 2 Two dangerous situations for people (including kids) visiting a glacier. In both cases, a sudden collapse of the ice vault or surface would involve human beings in the area



obtain a complete picture of the local conditions, including *digital surface models* (DSM) from photogrammetric and laser scanning techniques, ice-penetrating data, rheological and weather records, and measurement of sub-glacial water flow. In particular, the integration of surface and subsurface surveying and inspections is expected to provide a better support to the hydraulic and structural modelling, as already achieved in other fields of the Geosciences, see Longoni et al. (2012).

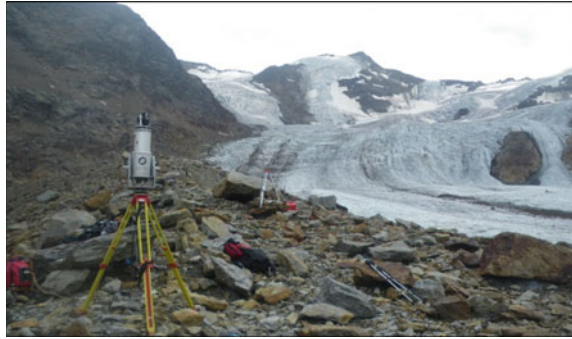
Among different types of observations from Remote Sensing (Rutzinger et al. 2018), DSM's play a paramount role because they help evaluate glacier thickness and volume variation, and to identify those areas where geomorphological and dynamical changes are expected (Kääb et al. 2005a). Provided that images at sufficient *ground sample distance* (GSD) are available, these may help the recognition of those typical hints of potential collapses, such as circular crevasses, sub-vertical ice walls, thin ice vaults and the like. The necessary GSD prevents the use of medium-resolution satellite images (e.g., ASTER, Landsat and Sentinel series), which are suitable for regional-scale mapping. Some authors have demonstrated that HR/VHR (high-resolution/very high-resolution) imagery may be exploited for investigating the majority of cryospheric hazards, see Kääb et al. (2005b) and Quincey et al. (2005). On the other hand, the analyses at the scale of single glaciers require higher resolution than the one that may be obtained only from specific airborne or ground missions employing Photogrammetry (image-based) or Laser Scanning (range-based). In addition, HR/VHR images may suffer from cloud cover and bad atmospheric conditions, that may result in difficulties in retrieval of suitable data sets.

It's out of the scope of this article to focus on pros vs contras of Photogrammetry (Luhmann et al. 2013) and Laser Scanning (Heritage 2009), which also depend on the specific application, see Chandler and Buckley (2016) and O'Banion et al. (2018). Photogrammetry, with the development of easy and accurate self-calibration techniques (Luhmann et al. 2016), Structure-from-Motion (SfM) for automatic image orientation (Barazzetti et al. 2009) and dense surface matching (Remondino et al. 2014) for detailed 3D reconstruction, has demonstrated to be a successful technique to be widely applied in the Geosciences (Eltner et al. 2016), among which high-mountain research (Remondino et al. 2014) and Glaciology (Piermattei et al. 2015, 2016). Nowadays, the term SfM Photogrammetry has become a synonym of the full automatic process leading to object reconstruction, not only limited to the orientation stage as in its origin (Hartley and Zisserman 2003).

A further help to the diffusion of SfM Photogrammetry has been the development of small UAV (Unmanned Aerial Vehicles or *drones*, see Sect. 2) for data acquisition (Santangelo et al. 2018). Regardless of the platform for image acquisition, ground-based or UAV Photogrammetry is quite flexible and does not call for the use of heavy equipment such in the case long/very-long range terrestrial laser scanners are used (see Fig. 3).

In the next Sect. 2, a review of the state-of-the-art of SfM Photogrammetry for application to glaciers is reported. In the following Sect. 3, a case study where the application of this technique has been carried to the study of changes of a glacier and to analyze the possible risks related to downwasting is presented and discussed.

Fig. 3 TLS acquisition at Forni Glacier (Raethian Alps, Italy) based on a *long-range terrestrial laser scanner Riegl LMS-Z420i*. Even though modern long-range and very long-range TLS have a smaller size and weight, they are still difficult to be carried and operated in high-mountain environment



2 SfM/UAV Photogrammetry in Glacier Studies

As already highlighted in Sect. 1, SfM Photogrammetry (Westoby et al. 2012; Granshaw 2018b) has given new popularity to the image-based reconstruction techniques after a period when Terrestrial Laser Scanning (TLS) seemed to become the main approach for 3D surface reconstruction. This success has been also supported by a large development of the applications in the domain of Geosciences, as widely reviewed in Eltner et al. (2016) and, recently, in O'Banion et al. (2018). But it is the combination of SfM and UAV's—also often referred to with many other acronyms, see the interesting discussion in Granshaw (2018a)—that transformed the photogrammetric technique in a competitive approach with respect to TLS for 3D reconstruction in the mountain environment (Ryan et al. 2015) and to face with emergency surveying during geohazards (Giordan et al. 2018). In addition to the lower cost, the SfM and UAV coupling allows to overcome the problems of occlusions and may simplify data acquisition in complex terrains as well, see Chandler and Buckley (2016). The road map to this success has been completed by the availability of several software packages implementing SfM in a user-friendly environment while keeping low-cost or also the availability of software from the open source community (Gonzalez-Aguilera et al. 2018).

Beyond the abovementioned reviews, different technical aspects about the use of integrated SfM/UAV Photogrammetry in Geosciences can be found in the literature: problems related to camera set up (Mosbrucker et al. 2017; O'Connor et al. 2017), mission planning (Pepe et al. 2018), direct georeferencing (Carbonneau and Dietrich 2017; Dall'Asta et al. 2017), evaluation of the accuracy using a theoretical framework (James et al. 2017) or an empirical approach (O'Banion et al. 2018), analysis of multi-temporal surveying reproducibility (Clapuyt et al. 2016).

In the field of *glaciological studies*, the potential of SfM/UAV Photogrammetry is documented in several applications. Glaciers in different areas of the Earth could be mapped, such as Svalbard Glaciers (Norway—Solbø and Storvold 2013), Fountain Glacier in Bylot Island (Canada—Whitehead et al. 2013), Forni Glacier in Raethian Alps (Italy—Fugazza et al. 2015, 2018), debris-covered Lirung glacier (Himalaya, Nepal—Immerzeel et al. 2014), calving dynamics at Store Glacier

(Greenland—Ryan et al. 2015), ice cliffs at Kilimanjaro Mount (Kenya—Winkler et al. 2012), and Gran Sommetta Glacier in Aosta Valley (Italy—Dall’Asta et al. 2017). The same approach may be used for mapping periglacial areas or moraines, as described in Tonkin et al. (2014), or to measure snow depth (Bühler et al. 2015). UAV’s may be used also to operate other types of remote sensing techniques, as discussed in Bhardwaj et al. (2016). In Kraaijenbrink et al. (2016) the emphasis is given to the application of *object-based image analysis* (OBIA) obtained from SfM/UAV Photogrammetry to map and characterize surface features (ponds, ice cliffs) on Langtang debris-covered glacier in Nepal.

For some applications the individual use of SfM Photogrammetry from ground-based stations may suffice to obtain the reconstruction of the glacier surface. This especially holds in the case of small glaciers (Piermattei et al. 2015, 2016) and where the local topography allows to set up a suitable network geometry from the ground (Gómez-Gutiérrez et al. 2014, 2015). In Fugazza et al. (2018) the integration of UAV/SfM and ground-based SfM Photogrammetry has been carried out to obtain a more complete 3D reconstruction of an Alpine glacier, as also shown in next Sect. 3.

3 A Case Study: The Forni Glacier in Raethian Alps, Italy

3.1 Case Study Presentation

A typical case where a rapid retreat is occurring with the development of local collapse processes in the ice-tongue terminus is given by the *Forni Glacier*, which is located in the Raethian Alps within the Ortles Cevedale mountain group. The glacier is included in the National Stelvio Park (Northern Italy). It is one of the major valley glaciers in the Italian Alps, which is currently suffering from intense ablation processes. The latest Italian Glacier Inventory (Smiraglia et al. 2015) reported the total glacier area as 11.34 km², an altitudinal range between 2501 and 3673 m a.s.l., and a North-North-Westerly aspect. Since this inventory was based on 2007 data, the successive separation of the multiple ice tongues, the loss of ice bulk at global level and the retreat resulted in a reduction of the reported extension. These are progressive processes that have been active in the latest decades but recently they have been showing a rapid acceleration. Just to give an idea of the magnitude of the retreat process, during the Little Ice Age (LIA), which approximately extended between 1500 and 1850 A.D., Forni Glacier spanned over an area of 17.80 km² (Diolaiuti and Smiraglia 2010). On the other hand, some sectors of the lower part of glacier’s main tongue are undergoing a local disruption process entailing first the formation of circular crevasses, to be followed by their collapse and the formation of large exposures of bedrock, see Fig. 4.

Other similar processes are documented in the literature (Albers et al. 2017). Such local processes are quite fast to develop: from their preliminary events to the full ice collapse the process may take less than one year. Monitoring the ice

Fig. 4 Examples of local collapses in the terminus area of Forni Glacier. From top to bottom: collapse of circular crevasses in 2016; the same process on the opposite side of the ice tongue in the end of Summer 2017 (after formation) and one year after (August 2018); the remaining right part of the glacier front after the creation of the discontinuity shown above



degradation process from a quantitative and qualitative point-of-view is of great importance to understand the related dynamics and to apply rigorous numerical models. While the analysis of archive maps, medium resolution satellite images and *digital elevation models* (DEM) may provide an overview of the long-term processes, as shown in Fig. 4, the application of close-range sensing techniques (Remondino et al. 2014) from ground-based and UAV stations offers the unprecedented opportunity to operate a 4D reconstruction of the glacier geometry at

both global and local levels. Recent research on this glacier can be found in Fugazza et al. (2015, 2016, 2018).

In the latest years, the melting process at Forni Glacier has resulted in the formation of some circular deep crevasses on the surface of the terminal ice tongue. Due to the contemporary erosion of subglacial water, large areas have collapsed resulting in the formation of huge craters in the ice tongue, see Fig. 4. The event occurred at the end of Summer 2017 (see Figs. 4 and 5) partially interrupted the active ice flow on the right hydrographic flank of the terminus, speeding up the melting process of this portion of the glacier.

In Fig. 5 a series of medium resolution satellite images (Sentinel 2A/2B) over the area of Forni Glacier has been used to provide an overview of the evolution of the retreat in the period that is considered here. Despite of the quite large GSD (10 m), these images allow to understand the formation and development of the local collapses close to the terminus of the glacier tongue.

In order to carry out a detailed analysis of the dynamic development of this glacier, the authors have decided to start some observation campaigns during the summer period, when the glacier is easier to be accessed and the melting process reaches its fastest rate. Missions using drones have been operated in 2014, 2016, 2017 and 2018. Starting in 2016, close-range photogrammetric surveys were accomplished from ground stations, in order to integrate some better views of vertical and subvertical facies that cannot be completely seen from vertical photos captured by drones. As reported in Fugazza et al. (2018) a comparative study between long-range TLS, UAV and terrestrial photogrammetry, was operated during the 2016 campaign. The results published there demonstrated that the integration of photogrammetry from both platforms may lead to adequate results for the purpose of this study, avoiding the necessity of using a TLS for the study of the ice tongue area. The DEM's derived from the interpolation of point clouds could be used for analyzing the rate of glacier retreat, the ice volume thickening and the consequent loss of water equivalent volume. The point clouds could be exploited for a better detection of the collapsed areas and to locate those regions where new forthcoming failures may be predicted.

In the next subsections, some aspects related to photogrammetric data acquisition at Forni Glacier case study are reported and discussed.

3.2 Photogrammetric Data Acquisition

3.2.1 UAV Missions

Four UAV missions covering the glacier terminus were operated from 2014 to date. The main technical features of these missions are reported in Table 1. The first survey covered both the terminus of the central and eastern ablation tongue of the glacier (see Fugazza et al. 2015). It was flown on 28th August 2014 using a SenseFly SwingletCam fixed wing aircraft at a relative flying height of

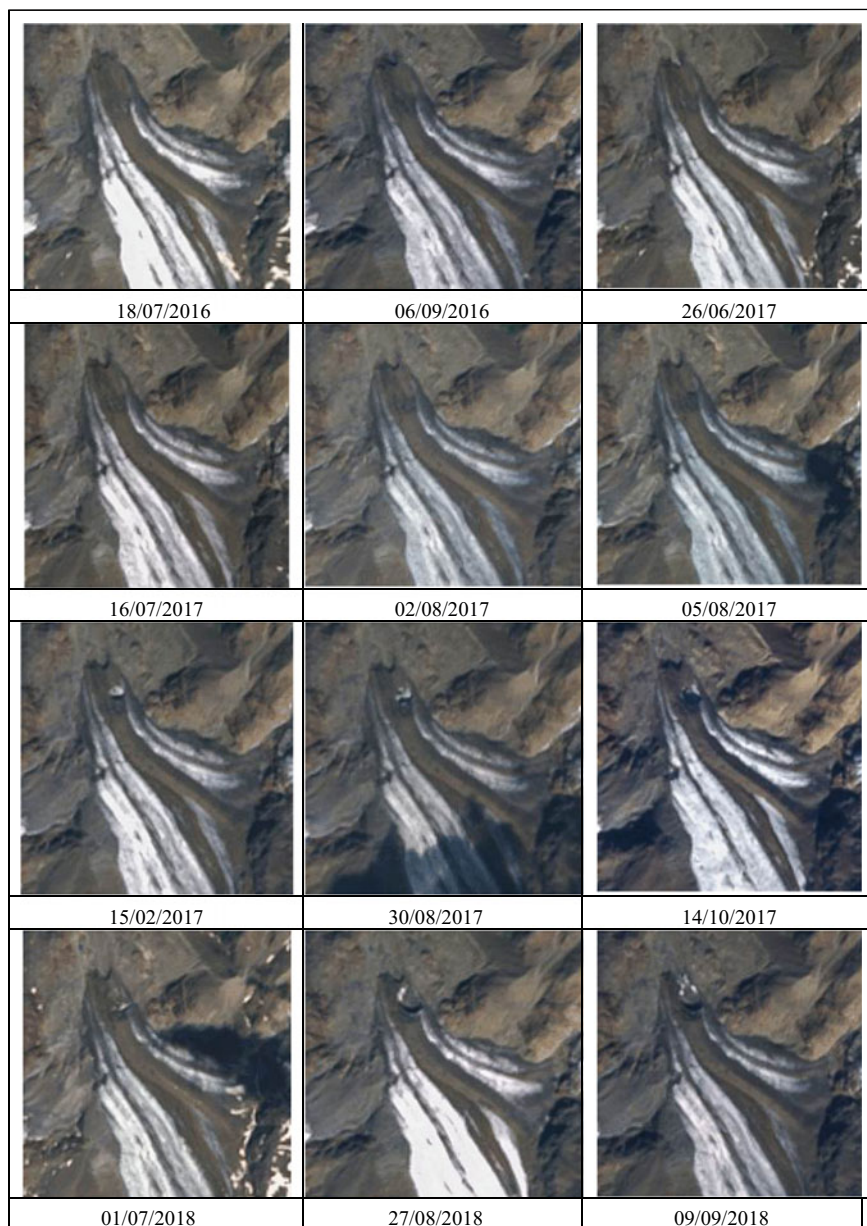


Fig. 5 Patches from Sentinel 2A/2B medium resolution satellite images (GSD = 10 m) depicting the dynamical evolution of the Forni Glacier's tongue from summer 2016 to summer 2018

Table 1 Main technical features of UAV mission at Forni Glacier from 2014–2018

UAV platform type	Time	UAV model	Camera model	Sensor size (pixels/mm)	Focal length (mm)	Avg. GSD (cm)	# GCP's
Fixed wing	08/2014	SwingletCam (SenseFly)	Canon IXUS 127 HS	4608 × 3456 6.16 × 4.62	4.3	12	0
Multicopter	08/2016	Customized quadcopter	Canon PowerShot ELPH 320 HS	4608 × 3456 6.16 × 4.62	4.3	6	8
Multicopter	10/2017	Customized quadcopter	Canon PowerShot ELPH 320 HS	4608 × 3456 6.16 × 4.62	4.3	5	5
Multicopter	08/2018	Customized quadcopter	Canon PowerShot ELPH 320 HS	4608 × 3456 6.16 × 4.62	4.3	6	6

approximately 380 m above the average glacier surface. The resulting average GSD was 12 cm. No *ground control points* (GCP's) were deployed during this flight. The only information available for absolute georeferencing were the 291 camera-pose locations obtained from the onboard navigation-grade GNSS (Global Navigation Satellite System) sensor. The uncertainty of this type of positioning could be estimated in the order of ± 2 m.

The second flight was operated across two days (30th August and 1st September 2016), see Fugazza et al. (2018). The drone employed in this mission was a customized quadcopter, flown at a low relative altitude of 50 m with respect to the topographic surface (average GSD = 6 cm). Eight GCP's were deployed on the glacier terminus and in the periglacial area in front of it. GCP coordinates were measured by using a GNSS/RTK (Real-Time Kinematic) sensor.

The third flight was operated on 25th October 2017 in order to reconstruct the glacier topography after the collapse occurred at the end of summer, see Fig. 4. The drone employed in this mission was a customized quadcopter. A GSD = 5 cm was achieved. A set of 5 GCP's measured using GNSS/RTK were used for georeferencing. The RMSE (Root Mean Square Error) on these residuals was evaluated as 7 cm.

A fourth flight was carried out during August 2018, but at the moment of writing the processing has not been completed yet.

3.2.2 Terrestrial Photogrammetric Campaigns

Three photogrammetric campaigns using digital cameras for the acquisition of images from ground-based stations around the glacier tongue have been accomplished up until today. The main characteristics of these blocks are shown in Table 2, while the locations of camera stations are illustrated in Fig. 6.

Table 2 Main technical features of terrestrial photogrammetric blocks captured at Forni Glacier from 2016–2018 (CST = camera stations)

Time	Camera model	Sensor size (pixels/mm)	Focal length (mm)	#GCP's
08/2016	Nikon D700	4256 × 2823/36 × 24	50	7
09/2017	Nikon D700	4256 × 2823/36 × 24	35	0
08/2018	Nikon D700	4256 × 2823/36 × 24	50	3 + 28 CST's

The first block was captured concurrently to the 2016 UAV mission. A block of 134 images captured using an SLR (single lens reflex) camera Nikon D700 equipped with 50 mm lens was obtained to cover the glacier terminus including the rock flanks, a part of the periglacial area, and the ending part of the central moraine over the main glacier tongue. The criterion applied for establishing the camera stations was to explore as many positions as possible from which the targeted region could be observed from multiple, redundant viewpoints. In particular, to optimize the SfM process for automatic image orientation, an attempt to find a trade-off between long baselines with convergent images (providing a better geometric intersection of corresponding rays) and short-baselines with parallel images (helping the image-matching process adopted for image orientation and surface reconstruction), see Wenzel et al. (2013). Seven natural features were selected as GCP's on the glacier front for georeferencing of terrestrial block. Their coordinates in the mapping reference frame were measured using a theodolite equipped with a reflector-less rangefinder. The position and heading of the theodolite stations in the geodetic reference frame was found using GNSS/RTK.

During September 2017, a new photogrammetric survey from ground-based stations was repeated after the impressive collapse shown in Fig. 4. A Nikon D700 camera equipped with 35 mm lens was adopted in such a case with the purpose of shortening the acquisition distance. This solution was necessary because of the geometric constraints imposed by the new collapse. Due to some technical problems, no measurements for absolute georeferencing could be obtained from this campaign.

The third available photogrammetric survey was operated at the beginning of August 2018. In such a case, the same SLR camera Nikon D700 equipped with a 50 mm lens was used. The location of a subset of camera stations were measured using GNSS/RTK to establish the ground reference datum. Additionally, a few rock features were also measured by GNSS/RTK to be recognized in photos and used as standard GCP's.

3.3 Photogrammetric Data Processing

The processing of all photogrammetric blocks from either terrestrial or UAV imaging platforms has been carried out by applying the same processing workflow.

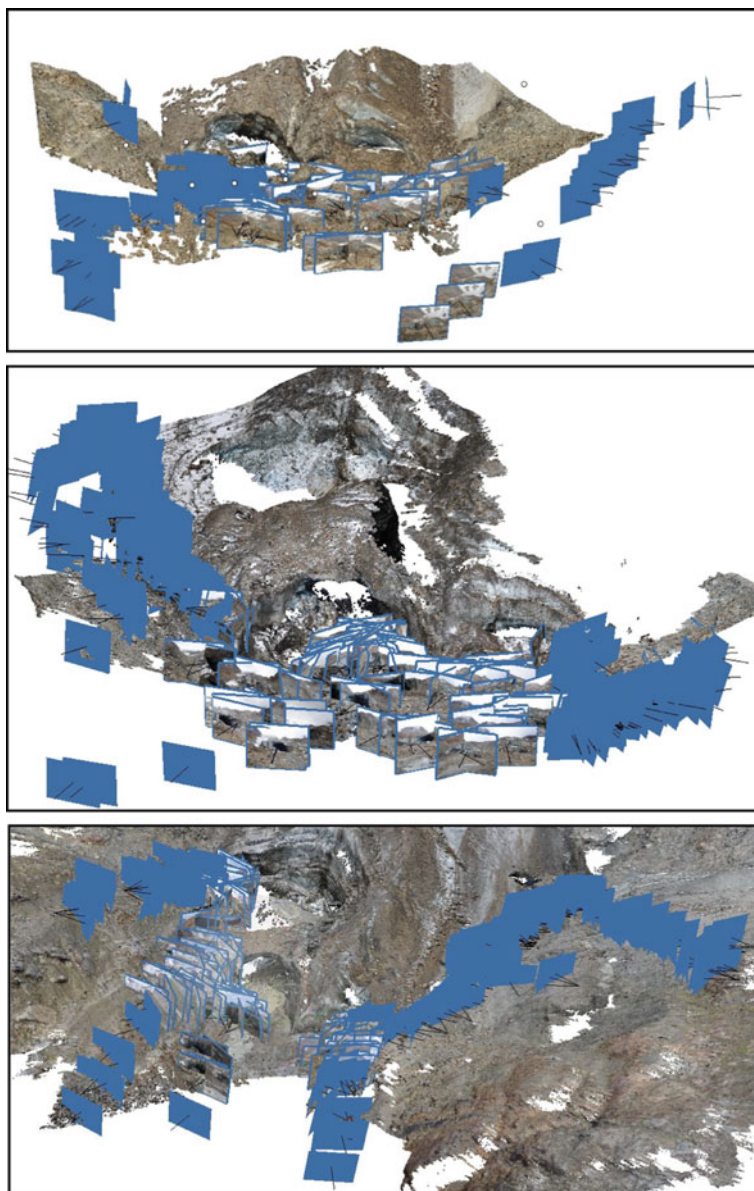


Fig. 6 Camera stations (blue rectangles) after exterior orientation of terrestrial photogrammetric networks accomplished in 2016 (at the top), in 2017 (in the middle), and in 2018 (at the bottom)

Table 3 Main properties of SfM processing with Agisoft Photoscan (r) Professional of the photogrammetric blocks captured at Forni Glacier in the period 2014–2018

Imaging platform (UAV/ Terrestrial)	Time (month/ year)	#oriented photos	Image RMS residuals (pix)	Processing “Accuracy” level		Final point cloud size (#10 ⁶ points)
				EO	Dense matching	
UAV (fixed wing)	08/2014	86	0.5	High	High	55.7
Terrestrial	08/2016	134	0.8	Highest	High	27.7
UAV (multicopter)	08/2016	288	2.0	Highest	High	75.1
Terrestrial	09/2017	232	0.4	Highest	High	29.5
UAV (multicopter)	10/2017	161	1.4	Highest	High	55.7
Terrestrial	08/2018	291	0.4	Highest	High	70.0

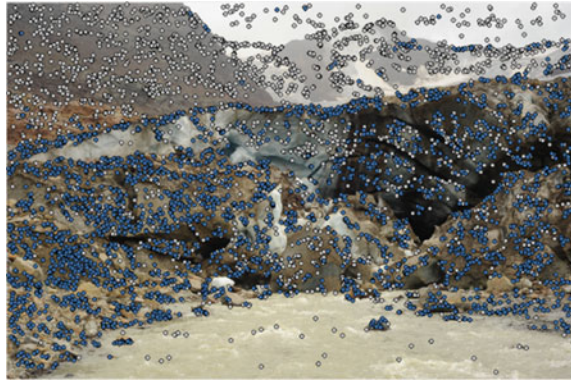
Each block has been independently processed. Agisoft Photoscan[®] Professional ver. 1.4.0 (in the following referred to as “APP”—www.agisoft.com) has been used for photogrammetry processing based on SfM and dense matching. The fusion of data sets captured at the same epoch has been carried out on the final point clouds in CloudCompare environment (www.cloudcompare.org). More details about the different processing stages are described in the following paragraphs. In Table 3, some basic properties of different processing steps adopted with these blocks are reported.

3.3.1 Sensors Calibration and Orientation

First, *tie points* (TP’s—Hartmann et al. 2016) have been extracted and matched using feature-based matching (FBM—Barazzetti et al. 2009). In Fig. 7, a typical distribution of feature points extracted as candidates for the FBM are displayed. Among these, blue points are those that have been successfully matched in other images and consequently they may play as TP’s in successive bundle-block adjustment (BBA). As can be clearly seen, discarded feature points (grey circles) are mainly located on the background and on the water surfaces. Since TP’s on these areas are not likely to be selected a mask could be applied to avoid it. On the other hand, this kind of filtering operation is difficult to automate, and masking should be manually applied to each photo. To escape this time-consuming operation, masking has not been considered, but we relied on the sufficient robustness of the TP set to discard points in unwanted areas. Barring a few exceptions, this strategy worked well, as shown in the example displayed in Fig. 7.

The BBA implemented in APP provided the exterior orientation (EO) of the images, the ground coordinates of TP’s, and camera calibration parameters. APP is able to compute all the approximate values of the unknown parameters needed to

Fig. 7 Example of feature points extracted on one image from terrestrial block captured in 2016: blue points represent TP's that have been matched in at least another image; grey points are features points that have not been successfully matched



instantiate the BBA, though providing initial values may speed up processing. This option has been followed in the case of the UAV blocks, since the GNSS onboard sensors recorded the position of each shot at navigational accuracy (approximately ± 2 m). In such a case, GNSS coordinates were used to instantiate the datum for the initial BBA. In the case of terrestrial blocks, no approximate values were available to help BBA processing. Anyway, the procedure could automatically derive the final EO parameters by using an internal strategy based on a preliminary SfM procedure carried out on subsampled images. Initial EO obtained this way was then used to instantiate the final processing. APP allows to define the level of accuracy (see Table 3). In most cases, the highest level has been selected (“Very-high accuracy”) in order to better define the EO of each block, which may guarantee a geometric stability to next processing steps. This level corresponds to processing the images at full resolution.

In the case of UAV blocks (2014, 2016, 2017) all the images could be processed at the same time, after discarding a few photos with significant shadows or wrong expositions (e.g., due to clouds). In the case of terrestrial blocks collected in 2016 and 2017, the direct processing of all the images together was not possible. Consequently, the block from 2016 was initially split into two sub-blocks (referred to as “chunks” in APP jargon) to be independently oriented. The block from 2017 required the subdivision in four sub-blocks. The standard procedure to join sub-blocks should be based on the use of a sufficient number of GCP's (Barazzetti et al. 2011), solution that could not be applied in such a case. Then sub-blocks were successfully merged using an automatic function implemented in APP with the purpose of aligning overlapping “chunks.” A critical analysis of this problem led to the conclusions that in the case of complex, large blocks, the overlaps between photos covering surfaces with a different spatial orientation should receive much attention during data acquisition. Thanks to this lesson learnt, the terrestrial block surveyed during August 2018 could be entirely oriented in a single step. In previous papers, some aspects such as the image configuration for the terrestrial blocks have been discussed, see Corti (2017), Fugazza et al. (2018), Scaioni et al. (2017). In Fig. 6 the camera poses for the terrestrial blocks are depicted.

3.3.2 Ground Control

In order to make sound comparisons among multi-temporal data sets, an external datum has been defined per each photogrammetric block. The planimetric datum adopted for georeferencing all mapping products in this part of Italy is ITRS2000/UTM 32 N.

Thanks to the measurements of static GNSS baselines with respect to permanent stations located at a distance inferior to 30 km, the accurate position of one or more GNSS/RTK master station in ITRS2000/UTM 32 N reference system was found. From here, differential corrections were broadcasted via radio-link to correct the position of a rover station used to determine the coordinates of targets to be used as GCP's in UAV projects. In other cases, the GNSS/RTK rover was used to measure directly the camera stations of photogrammetric blocks, or some vertices from which theodolite measurements could be operated. In the case of terrestrial blocks, either targets and natural features were used as GCP's.

Since GNSS processing could provide ellipsoidal elevations, each project needed to be transformed into orthometric heights. In order to have a standard procedure for determining local geoid undulation and due to the limited size of the area where the glacier terminal tongue spanned over, a unique constant value was selected. The constant undulation was computed with the help of the official software Verto 3, distributed by the Italian mapping agency (IGMI).

When enough GCP's were available, these have been directly included in the BBA implemented in APP to establish the geodetic *datum*. GCP's can be included as weighted pseudo-observations, contributing this way to adjust possible geometric deformations of the block. In fact, in most SfM software packages, GCP's are only used to compute a general 3D similarity transformation to better fit GCP coordinates in object space to corresponding coordinates derived from space intersection. In general, a limited number (less than ten) GCP's were available per each project. Average residuals on GCP's resulted in the order of few tens of centimetres. These results are aligned with the ones obtained in similar projects on other glaciers (see, for example, Piermattei et al. 2015, 2016).

In the case of missing sufficient GCP's, some alternative procedures were applied to align a block with respect to another one already georeferenced in ITRS2000/UTM 32 N. When two blocks collected at the same time (or at short time gap) had to be oriented, they were first imported into the same APP project as "chunks." Then the procedure for merging "chunks" on the basis of FBM was applied. This was the case, for instance, of the terrestrial block collected in 2017, for which it was not possible to measure any GCP's due to the time shortage during data acquisition campaign. In such a case, the UAV block flown during the same year was used as reference for co-registration, since in the case of this block a consistent set of GCP's was available.

On the other hand, in the case of the co-registration of blocks captured in different years, the same procedure could not be used because of the impressive changes of the local surface. Indeed, it is really difficult to find persistent features to be used for co-registration when a full year has passed: in addition to the ice flow

and melting, also the periglacial area in front of the glacier may undergo dramatic changes, while the surface texture may be completely altered due to the action of atmospheric agents. In such a case, the 3D coordinates of GCP's can be derived by spatial intersection from the already oriented images of the block to be used as reference. These "photogrammetric" GCP's should be selected in correspondence of selected features that may be easily recognized at both epochs in stable areas (for example on the rocks outside the glacier tongue). The number of these GCP's should be sufficient to guarantee a stable geometry in the registration process, and to maintain enough precision. In the case the identification of "photogrammetric" GCP's is difficult, another approach consists in including some images from the block to be registered into the reference block. Once this new data set is oriented using SfM, the image coordinates of "photogrammetric" GCP's can be measured in the same images for the both blocks. Then the EO of the reference block will be used to compute the object coordinates of GCP's to be used for co-registration of the other block (Scaioni et al. 2017).

3.3.3 3D Reconstruction Using Dense Surface Matching

A dense matching technique has been adopted for deriving the point cloud describing the surface of the region of interest. The "Build Dense Cloud" function implemented in APP has been used to this purpose. In Table 3 the main input parameters and some characteristics of the output point clouds are shown for all data sets. In all of them, the total number of images could be processed at the same time starting from the EO and camera calibration parameters that had been previously computed. The "High" accuracy level has been set up, which is based on subsampled images at half the original resolution. As discussed in Scaioni et al. (2017), the use of the images at full resolution ("Very-high" accuracy level) entails an impressive growth of processing time and computing resources, which is not counterbalanced by the increase of quality in the final point cloud. In addition, the size of this may become too large so that a successive decimation filtering might be necessary to handle such a huge data set. The final point clouds have been automatically assigned colors to points by using RGB information from images.

3.4 Data Fusion

Point clouds from "terrestrial" and "UAV" blocks collected during 2017 campaigns are displayed in Fig. 8 to show differences. Similar figures may be retrieved in Fugazza et al. (2018) to show the same point clouds but from 2016 campaigns. In Fig. 9, a quantitative comparison between these point clouds is also reported. This has been carried out in CloudCompare environment using M3C2 function (Lague et al. 2013).

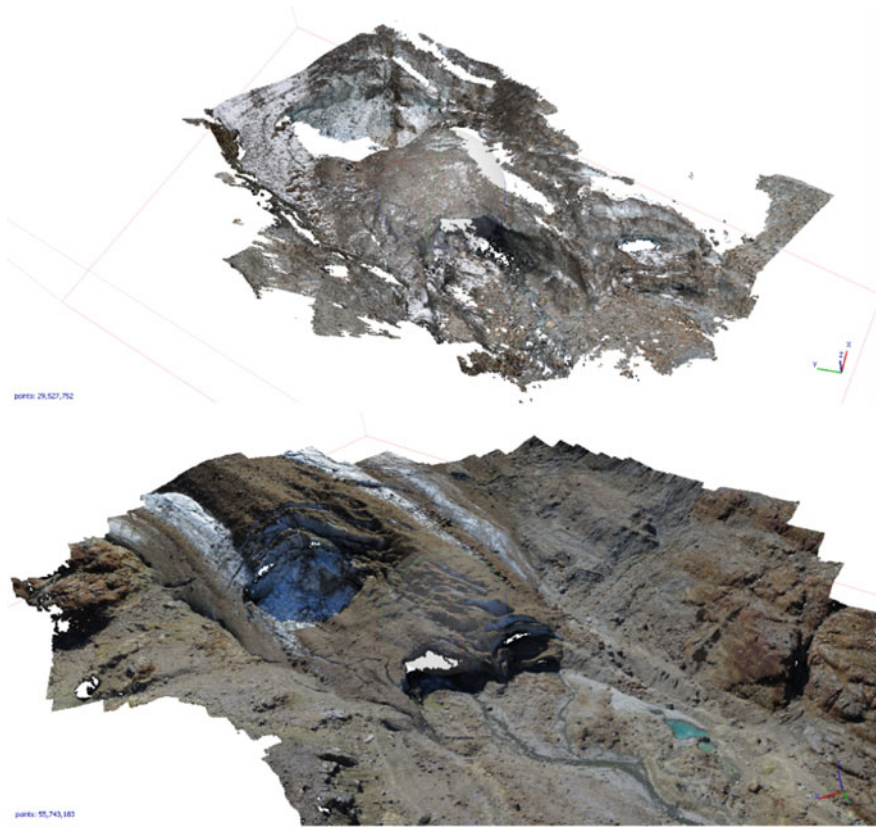


Fig. 8 Point clouds obtained from “terrestrial” (at the top) and “UAV” (at the bottom) blocks captured in 2017

While for some applications a single point cloud per epoch (from UAV or from ground-based stations) may suffice, the data fusion of both may lead to a more complete 3D reconstruction. Thanks to previous georeferencing into the same reference system, point clouds could be directly merged. Afterwards, the resulting data sets were subsampled at 20 cm spatial resolution to obtain complete 3D reconstruction of the entire ice tongue of the Forni Glacier in 2016 and 2017, see Figs. 10 and 11, respectively. RGB information of points in overlapping areas has been also averaged. Indeed, due to the large size of the merged point clouds, to the high point density in the overlapping regions, and the possible presence of small misalignments at local level, subsampling allowed overcoming all these drawbacks. Furthermore, the resulting point clouds were easier to handle.

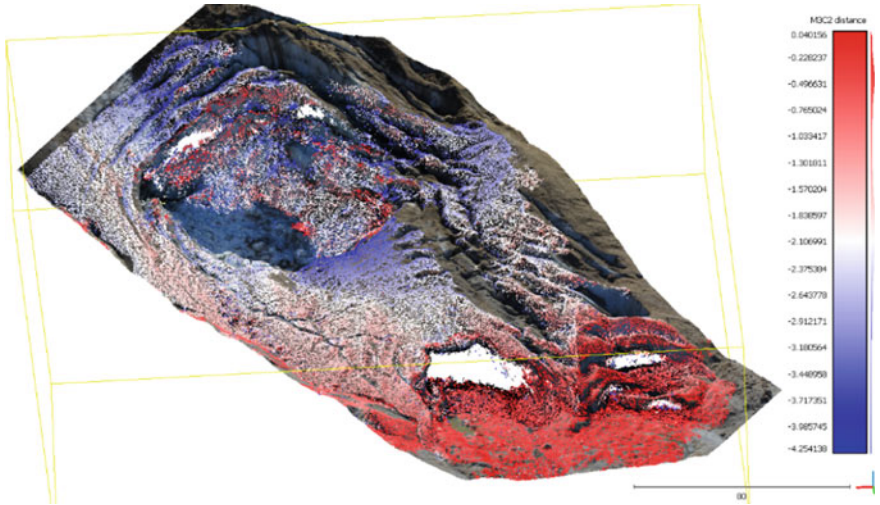


Fig. 9 Comparison between point clouds obtained from “terrestrial” and “UAV” blocks captured in 2017 (see Fig. 8). Grey areas are those where no overlap exists

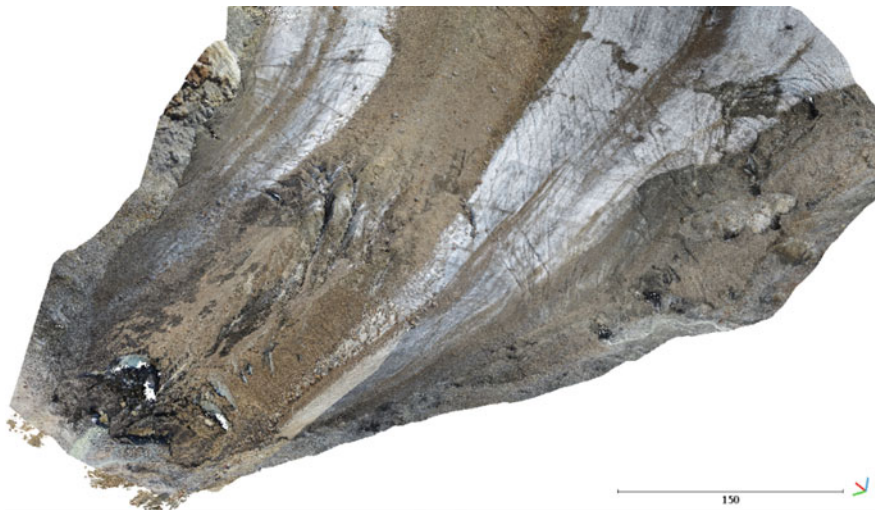


Fig. 10 Point cloud obtained from the fusion of “terrestrial” and “UAV” blocks captured in 2016

The integration of a point cloud obtained from airborne vertical images to another one from ground-based camera stations, allows to improve the reconstruction of surfaces with different spatial orientation such as those typical of a glacier terminus.

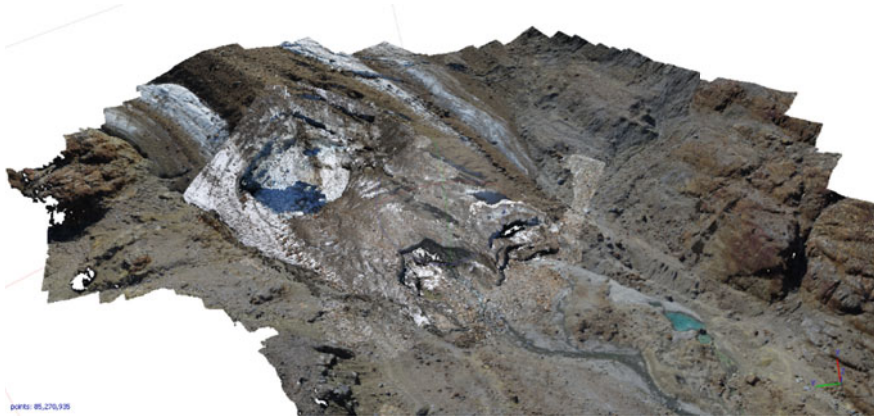


Fig. 11 Point cloud obtained from the fusion of “terrestrial” and “UAV” blocks captured in 2017

3.5 Results and Discussion

The point cloud obtained by merging terrestrial and UAV blocks captured in 2016 (Fig. 10) covers the full terminus of the Forni Glacier. In addition, no holes or major occlusions can be noticed. By looking at 3D geometry, the presence of surface features is easy to detect. The presence of a large collapsed area (Summer 2016) on the left hydrographic side of the glacier can be observed.

The point cloud derived from terrestrial and UAV blocks surveyed during September 2017 (Fig. 11) has a smaller spatial coverage. It should be also remarked that the complexity of the glacier topography was higher in 2017, due to the large area that collapsed in the end of summer, and the major fragmentation of the terminus. Anyway, these events are clearly visible in the point cloud, also because data acquisition was designed for their specific documentation.

By looking at point clouds from 2016 and 2017, a first impressive change concerned the interannual retreat of the glacier front. The average value distance between the medial part of the front was 38 m. The observed shape of the front is quite similar in both years, with the terminus split in two longitudinal sectors by the medial supraglacial moraine. In both sectors, water may flow out from the glacier, where it is excavating subglacial tunnels. The thinning of the vault of a portion of the right tunnel was probably the causative reason of the collapse occurred in the end of summer 2017. This resulted in the formation of a big crater, which also had the effect of breaking the ice flow on the terminal part of the corresponding longitudinal sector, close to the glacier front. The lack of ice input will speed up the melting process of this part of the terminus.

In August 2018 the “terrestrial” point cloud shows a progress in the retreat of the glacier front, while the collapsed area continued to grow. It is interesting to notice that the water flow has now completely switched to the right hydrographic side, since no water is flowing out from the left side.

During each summer, the terminus of Forni Glacier is visited by many hikers and tourists. On one hand, tracks to reach some mountain peaks in the nearby go through the terminus. On the other hand, the short walking distance from Branca Hut, which may be also reached using a car service, brings hundreds of tourists every day to the terminus. The easy access allows also non-experts and children to visit this area. Consequently, big collapses like the ones discussed in this paper, and other of minor magnitude, may have serious consequences on people visiting the glacier.

The availability of 3D models obtained from photogrammetric surveys may help understand those areas where collapses are foreseen, and consequently to limit the access to the glacier. In particular, these 3D models may help obtain a three-dimensional view of the problems, and to realize which is the effective region involved. In addition, the use of stereo-visualization and virtual-reality techniques may help better understand the glacier morphology without a direct inspection of the site.

Of course, this type of information may be integrated by on-site reconnaissance and other investigations (weather conditions, precipitations, ice penetrating radar, hydraulic flow measurements, etc.).

Another option to consider consists in the installation of fixed cameras to record a continuous documentation of melting events. Thanks to suitable locations of at least two cameras, the stereo-reconstruction by using dense matching techniques could be operated (see Roncella and Forlani 2015). Terrestrial photogrammetric blocks could be exploited to help find the optimal positions for those camera stations, by means of some network simulations to evaluate the completeness and the accuracy of the obtainable point clouds.

Of course, in the future the availability of several 3D models that will be likely captured at least on an yearly basis is expected to provide a very detailed description of the ongoing processes. A better understanding on how they may dynamically evolve since the appearance of precursory signals on the glacier surface and whether there are some parameters that may be related to them, will potentially lead to a more precise forecasting of collapses and then to assess the risk for those people who visit the glacier. To this purpose, the repetition of more data acquisition campaigns during the same summer (e.g., on a monthly-basis), may provide unprecedented information to understand these rapid melting processes, to be generalized to other case studies as well.

4 Conclusions

The application of ‘Structure-from-Motion’ (SfM) Photogrammetry from ground-based and UAV imaging platforms has been evaluated for monitoring changes of mountain glaciers. In this paper the focus has been given on the assessment of the risk of collapses, which may potentially result in casualties among people who visit some glaciers. Even though the specific analyses for the

evaluation of the risk have not been directly in the scope of the paper, the availability of detailed 3D models of the glacier surface has been highlighted as a potential source of information for this type of investigations.

The paper has specifically dealt with the case study of Forni Glacier, where the risk is quite relevant under current global warming conditions and accelerated melting. In such a case, the use of SfM Photogrammetry has been demonstrated to be quite supportive, since the analysis and comparison of 3D models allowed to extract useful information to detect potential collapses.

Close-range surveys from drones and ground-based imaging platforms are supposed to be repeated in the future for both long-term (annual basis) and short-term (monthly basis, only during summer), to better depict global and local phenomena contributing to the acceleration of the glacier ablation process. Since a measurement campaign requires time, suitable weather conditions, and a team of people, the organization of multiple expeditions is in general a non-trivial task. For this reason, on one side the installation of a permanent camera system for both visual analysis and 3D reconstruction is envisaged. On the other side, SfM Photogrammetry is now mature to be implemented within Citizen Science initiatives, for instance. People may be trained on how and where images should be collected, while the processing stage may be left to experts. As proposed in Albers et al. (2017), some apps may be also developed to guide users to capture the images following a precise scheme and to obtain redundant data acquisition.

Acknowledgements This study was funded by DARA (Department for regional affairs and autonomies) of the Presidency of the Council of the Italian Government). The authors acknowledge the Central Scientific Committee of CAI (Italian Alpine Club) and Levissima San Pellegrino S.P.A. for funding the UAV quadcopter. The authors also thank Stelvio Park Authority for the logistic support and for permitting the UAV surveys. The authors would also like to acknowledge those colleagues, students and friends who helped with different stages of field operations. In particular Manuel Corti and Julián Crippa.

References

- Albers B, De Lange N, Xu S (2017) Augmented citizen science for environmental monitoring and education. *Int Arch Photogramm Remote Sens Spatial Inf Sci* 42(2/W7):1–4. <https://doi.org/10.5194/isprs-archives-xlii-2-w7-1-2017>
- Barazzetti L, Forlani G, Remondino F, Roncella R, Scaioni M (2011) Experiences and achievements in automated image sequence orientation for close-range photogrammetric projects. In: *Videometrics, range imaging, and applications XI*. International Society for Optics and Photonics, paper no. 80850F. <https://doi.org/10.1117/12.890116>
- Barazzetti L, Remondino F, Scaioni M (2009) Combined use of photogrammetric and computer vision techniques for fully automated and accurate 3D modeling of terrestrial objects. In: *Videometrics, range imaging, and applications X*. International Society for Optics and Photonics, paper no. 74470 M. <https://doi.org/10.1117/12.825638>
- Bhardwaj A, Sam L, Martín-Torres FJ, Kumar R (2016) UAVs as remote sensing platform in glaciology: Present applications and future prospects. *Remote Sens Env* 175:196–204. <https://doi.org/10.1016/j.rse.2015.12.029>

- Bühler Y, Marty M, Egli L, Veitinger J, Jonas T, Thee P, Ginzler C (2015) Snow depth mapping in high-Alpine catchments using digital photogrammetry. *Cryosphere* 9:229–243. <https://doi.org/10.5194/tc-9-229-2015>
- Carbonneau PE, Dietrich JT (2017) Cost-effective non-metric photogrammetry from consumer-grade SUAS: implications for direct georeferencing of structure from motion photogrammetry. *Earth Surf Proc Land* 42(3):473–486. <https://doi.org/10.1002/esp.4012>
- Carey M, McDowell G, Huggel C, Jackson J, Portocarrero C, Reynolds J M, Vicuña L (2015) Integrated approaches to adaptation and disaster risk reduction in dynamic socio-cryospheric systems. In: Shroder JF, Haeberli W, Whiteman C (eds) *Snow and ice-related hazards, risks and disasters*. Academic Press, Elsevier, pp 219–261. <https://doi.org/10.1016/B978-0-12-394849-6.00008-1>
- Chandler JH, Buckley S (2016) Structure from motion (SfM) photogrammetry vs terrestrial laser scanning. In: Carpenter MB, Keane CM (eds) *Geoscience handbook 2016: AGI data sheets*, 5th edn. American Geosciences Institute, Alexandria (Virginia-USA), p 4
- Clapuyt F, Vanacker V, Van Oost K (2016) Reproducibility of UAV-based earth topography reconstructions based on structure-from-motion algorithms. *Geomorph* 260:4–15. <https://doi.org/10.1016/j.geomorph.2015.05.011>
- Corti M (2017) Analysis of multiple data sources for topographic reconstruction of Forni Glacier (Rhaetian Alps, Italy). Dissertation, Politecnico di Milano, MSc on Civil Engineering for Risk Management
- Dall'Asta E, Forlani G, Roncella R, Santise M, Diotri F, Di Cella UM (2017) Unmanned aerial systems and DSM matching for rock glacier monitoring. *ISPRS J Photogramm Remote Sens* 127:102–114. <https://doi.org/10.1016/j.isprsjprs.2016.10.003>
- Diolaiuti G, Smiraglia C (2010) Changing glaciers in a changing climate: How vanishing geomorphosites have been driving deep changes in mountain landscapes and environments. *Geomorphologie: relief, processus, environnement* 16(2):131–152. <https://doi.org/10.4000/geomorphologie.7882>
- Eltner A, Kaiser A, Castillo C, Rock G, Neugirg F, Abellán A (2016) Image-based surface reconstruction in geomorphometry—merits, limits and developments. *Earth Surf Dyn* 4:359–389. <https://doi.org/10.5194/esurf-4-359-2016>
- Fey C, Wichmann V, Zangerl C (2017) Reconstructing the evolution of a deep seated rockslide (Marzell) and its response to glacial retreat based on historic and remote sensing data. *Geomorphology* 298:72–85. <https://doi.org/10.1016/j.geomorph.2017.09.025>
- Fugazza D, Senese A, Azzoni RS, Smiraglia C, Cernuschi M, Severi D, Diolaiuti GA (2015) High-resolution mapping of glacier surface features. The UAV survey of the Forni glacier (Stelvio National Park, Italy). *Geogr Fis Din Quat* 38:25–33. <https://doi.org/10.4461/GFDQ.2015.38.03>
- Fugazza D, Senese A, Azzoni RS, Maugeri M, Diolaiuti GA (2016) Spatial distribution of surface albedo at the Forni glacier (Stelvio National Park, Central Italian Alps). *Cold Reg Sci Technol* 125:128–137. <https://doi.org/10.1016/j.coldregions.2016.02.006>
- Fugazza D, Scaioni M, Corti M, D'agata C, Azzoni RS, Cernuschi M, Smiraglia C, Diolaiuti GA (2018) Combination of UAV and terrestrial photogrammetry to assess rapid glacier evolution and map glacier hazards. *Nat Hazard Earth Sys Sci* 18:1055–1071. <https://doi.org/10.5194/nhess-18-1055-2018>
- Giordan D, Hayakawa Y, Nex F, Remondino F, Tarolli P (2018) The use of remotely piloted aircraft systems (RPASS) for natural hazards monitoring and management. *Nat Hazard Earth Sys Sci* 18:1079–1096. <https://doi.org/10.5194/nhess-18-1079-2018>
- Gobiet A, Kotlarski S, Beniston M, Beniston M, Heinrich G, Rajczak J, Stoffel M (2014) 21st Century climate change in the European Alps—A review. *Sci Total Environ* 493:1138–1151. <https://doi.org/10.1016/j.scitotenv.2013.07.050>
- Gómez-Gutiérrez Á, De Sanjosé-Blasco JJ, De Matías-Bejarano J et al (2014) Comparing two photo-reconstruction methods to produce high density point clouds and DEMs in the Corral del Veleta rock glacier (Sierra Nevada, Spain). *Remote Sens-Basel* 6(6):5407–5427. <https://doi.org/10.3390/rs6065407>

- Gómez-Gutiérrez Á, De Sanjosé-Blasco JJ, Lozano-Parra J, Berenguer-Sempere F (2015) Does HDR pre-processing improve the accuracy of 3d models obtained by means of two conventional SfM-MVS software packages? The case of the Corral del Veleta rock glacier. *Remote Sens-Basel* 7(8):10269–10294. <https://doi.org/10.3390/rs70810269>
- Gonzalez-Aguilera D, López-Fernández L, Rodríguez-Gonzálvez P, Hernández-López D, Guerrero D, Remondino F, Menna F, Nocerino E, Toschi I, Ballabeni A (2018) Graphos—open-source software for photogrammetric applications. *Photogramm Rec* 33:11–29. <https://doi.org/10.1111/phor.12231>
- Granshaw SI (2018a) RPV, UAV, UAS, RPAS ... or just drone? *Photogramm Rec* 33:160–170. <https://doi.org/10.1111/phor.12244>
- Granshaw SI (2018b) Structure from motion: origins and originality. *Photogramm Rec* 33:6–10. <https://doi.org/10.1111/phor.12237>
- Hartley R, Zisserman A (2003) *Multiple view geometry in computer vision*. Cambridge University Press, Cambridge
- Hartmann W, Havlena M, Schindler K (2016) Recent developments in large-scale tie-point matching. *ISPRS J Photogramm* 115:47–62. <https://doi.org/10.1016/j.isprsjprs.2015.09.005>
- Heritage GL, Large AGR (eds) (2009) *Laser scanning for the environmental sciences*. Wiley, Chichester, p 302
- Immerzeel WW, Kraaijenbrink PDA, Shea JM, Shrestha AB, Pellicciotti F, Bierkens MFP, De Jong SM (2014) High-resolution monitoring of Himalayan glacier dynamics using unmanned aerial vehicles. *Remote Sens Environ* 150:93–103. <https://doi.org/10.1016/j.rse.2014.04.025>
- James MR, Robson S, Smith MW (2017) 3-D uncertainty-based topographic change detection with structure-from-motion photogrammetry: Precision maps for ground control and directly georeferenced surveys. *Earth Surf Proc Land* 42:1769–1788. <https://doi.org/10.1002/esp.4125>
- Kääb A, Huggel C, Fischer L, Guex S, Paul F, Roer I, Salzmann N, Schläefli S, Schmutz K, Schneider D (2005a) Remote sensing of glacier-and permafrost-related hazards in high mountains: an overview. *Nat Hazard Earth Sys Sci* 5:527–554. <https://doi.org/10.5194/nhess-5-527-2005>
- Kääb A, Reynolds JM, Haeberli W (2005b) Glacier and permafrost hazards in high mountains. In: Huber UM, Bugmann HKM & Reasoner MA (eds) *Global change and mountain regions. Advances in Global Change Research, Vol 23*. Springer, Dordrecht, p 225. https://doi.org/10.1007/1-4020-3508-X_23
- Kerr RA (2012) Experts agree global warming is melting the world rapidly. *Science* 338 (6111):1138. <https://doi.org/10.1126/science.338.6111.1138>
- Kraaijenbrink P, Shea J, Pellicciotti F, De Jong S, Immerzeel W (2016) Object-based analysis of unmanned aerial vehicle imagery to map and characterise surface features on a debris-covered glacier. *Remote Sens Environ* 186:581–595. <https://doi.org/10.1016/j.rse.2016.09.013>
- Lague D, Brodu N, Leroux J (2013) Accurate 3D comparison of complex topography with terrestrial laser scanner: application to the Rangitikei Canyon (N-Z). *ISPRS J Photogramm* 82:10–26. <https://doi.org/10.1016/j.isprsjprs.2013.04.009>
- Longoni L, Arosio D, Scaioni M, Papini M, Zanzi L, Roncella R, Brambilla D (2012) Surface and subsurface non-invasive investigations to improve the characterization of a fractured rock mass. *J Geophys Eng* 9:461. <https://doi.org/10.1088/1742-2132/9/5/461>
- Luhmann T, Fraser C, Maas H-G (2016) Sensor modelling and camera calibration for close-range photogrammetry. *ISPRS J Photogramm* 115:37–46. <https://doi.org/10.1016/j.isprsjprs.2015.10.006>
- Luhmann T, Robson S, Kyle S, Boehm J (2013) *Close-range Photogrammetry and 3D Imaging*. Walter de Gruyter, p 684
- Mosbrucker AR, Major JJ, Spicer KR, Pitlick J (2017) Camera system considerations for geomorphic applications of SfM photogrammetry. *Earth Surf Proc Land* 42:969–986. <https://doi.org/10.1002/esp.4066>
- O’Banion MS, Olsen MJ, Rault C, Wartman J, Cunningham K (2018) Suitability of structure from motion for rock-slope assessment. *Photogramm Rec* 33:217–242. <https://doi.org/10.1111/phor.12241>

- O'Connor J, Smith MJ, James MR (2017) Cameras and settings for aerial surveys in the geosciences: optimising image data. *Prog Phys Geog* 41:325–344. <https://doi.org/10.1177/0309133317703092>
- Palomo I (2017) Climate change impacts on ecosystem services in high mountain areas: a literature review. *Mt Res Dev* 37:179–187. <https://doi.org/10.1659/MRD-JOURNAL-D-16-00110.1>
- Pepe M, Fregonese L, Scaioni M (2018) Planning airborne photogrammetry and remote-sensing missions with modern platforms and sensors. *Eur J Remote Sens* 51:412–435. <https://doi.org/10.1080/22797254.2018.1444945>
- Piermattei L, Carturan L, Guarnieri A (2015) Use of terrestrial photogrammetry based on structure-from-motion for mass balance estimation of a small glacier in the Italian Alps. *Earth Surf Proc Land* 40:1791–1802. <https://doi.org/10.1002/esp.3756>
- Piermattei L, Carturan L, De Blasi F, Tarolli P, Fontana GD, Vettore A, Pfeifer N (2016) Suitability of ground-based SfM-MVS for monitoring glacial and periglacial processes. *Earth Surf Dynam* 4:325–443. <https://doi.org/10.5194/esurf-4-425-2016>
- Quincey D, Lucas R, Richardson S, Glasser N, Hambrey M, Reynolds J (2005) Optical remote sensing techniques in high-mountain environments: application to glacial hazards. *Prog Phys Geog* 29:475–505. <https://doi.org/10.1191/0309133305pp456ra>
- Remondino F, Spera MG, Nocerino E, Menna F, Nex F (2014) State of the art in high density image matching. *Photogramm Rec* 29:144–166. <https://doi.org/10.1111/phor.12063>
- Roncella R, Forlani G (2015) A fixed terrestrial photogrammetric system for landslide monitoring. In: Scaioni M, (ed) *Modern technologies for landslide monitoring and prediction*, Springer, Cham. https://doi.org/10.1007/978-3-662-45931-7_3
- Rutzinger M, Bremer M, Höfle B, Hämmerle M, Lindenbergh R, Oude Elberink S, Pirotti F, Scaioni M, Wujanz D, Zieher T (2018) Training in innovative technologies for close-range sensing in alpine terrain. *ISPRS Ann Photogramm Remote Sens Spatial Inf Sci* 4(2):239–246. <https://doi.org/10.5194/isprs-annals-iv-2-239-2018>
- Ryan JC, Hubbard AL, Box JE, Todd J, Christoffersen P, Carr JR, Holt TO, Snooke NA (2015) UAV photogrammetry and structure from motion to assess calving dynamics at store glacier, a large outlet draining the Greenland ice sheet. *Cryosphere* 9:1–11. <https://doi.org/10.5194/tc-9-1-2015>
- Santangelo M, Alvioli M, Baldo M, Cardinali M, Giordan D, Guzzetti F, Marchesini I, Reichenbach P (2018) Brief communication: Remotely piloted aircraft systems for rapid emergency response: road exposure to rockfall in Villanova di Accumoli (Central Italy). *Nat Hazard Earth Sys Sci*. <https://doi.org/10.5194/nhess-2018-177> Accessed 18 Oct 2018
- Scaioni M, Corti M, Diolaiuti G, Fugazza D, Cernuschi M (2017) Local and general monitoring of Forni glacier (Italian alps) using multi-platform structure-from-motion photogrammetry. *Int Arch Photogramm Remote Sens Spatial Inf Sci* 42(2/W7):1547–1554. <https://doi.org/10.5194/isprs-archives-xlii-2-w7-1547-2017>
- Smiraglia C, Azzoni RS, D'agata C, Maragno D, Fugazza D, Diolaiuti GA (2015) The evolution of the Italian glaciers from the previous data base to the new Italian inventory. Preliminary considerations and results. *Geogr Fis Din Quat* 38:79–87. <https://doi.org/10.4461/GFDQ.2015.38.08>
- Solbø S, Storbø R (2013) Mapping Svalbard glaciers with the cryowing UAS. *Int Arch Photogramm Remote Sens Spatial Inf Sci* 40(1/W2):373–377. <https://doi.org/10.5194/isprsarchives-XL-1-W2-373-2013>
- Tonkin TN, Midgley NG, Graham DJ, Labadz J (2014) The potential of small unmanned aircraft systems and structure-from-motion for topographic surveys: a test of emerging integrated approaches at CWM Idwal, North Wales. *Geomorph* 226:35–43. <https://doi.org/10.1016/j.geomorph.2014.07.021>
- Wenzel K, Rothermel M, Fritsch D, Haala N (2013) Image acquisition and model selection for multi-view stereo. *Int Arch Photogramm Remote Sens Spatial Inf Sci* 40(5/W1):251–258. <https://doi.org/10.5194/isprsarchives-XL-5-W1-251-2013>

- Westoby MJ, Brasington J, Glasser NF, Hambrey MJ, Reynolds J (2012) 'Structure-from-Motion' Photogrammetry: a low-cost, effective tool for Geoscience applications. *Geomorph* 179:300–314. <https://doi.org/10.1016/j.geomorph.2012.08.021>
- Whitehead K, Moorman B, Hugenholtz C (2013) Brief communication: low-cost, on-demand aerial Photogrammetry for glaciological measurement. *Cryosphere* 7:1879–1884. <https://doi.org/10.5194/tc-7-1879-2013>
- Winkler M, Pfeffer WT, Hanke K (2012) Kilimanjaro ice cliff monitoring with close range photogrammetry. *Int Arch Photogramm Remote Sens Spatial Inf Sci* 39(B5):441–446. <https://doi.org/10.5194/isprsarchives-XXXIX-B5-441-2012>